Title

Metabolism of 2,2',3,3',6,6'-hexachlorobiphenyl (PCB 136) atropisomers in tissue slices from phenobarbital or dexamethasone-induced rats is sex-dependent.

Journal

Xenobiotica; the fate of foreign compounds in biological systems, 43(11)

ISSN

0049-8254

Authors

Wu, Xianai
Kania-Korwel, Izabela
Chen, Hao
et al.

Publication Date

2013-11-01

DOI

10.3109/00498254.2013.785626

Peer reviewed

http://informahealthcare.com/xen
ISSN: 0049-8254 (print), 1366-5928 (electronic)

Xenobiotica

Xenobiotica, Early Online: 1–15
 DOI: 10.3109/00498254.2013.785626

informa
healthcare

RESEARCH ARTICLE

Metabolism of 2,2′,3,3′,6,6′-hexachlorobiphenyl (PCB 136) atropisomers in tissue slices from phenobarbital or dexamethasone-induced rats is sex-dependent

Xianai Wu[1], Izabela Kania-Korwel[1], Hao Chen[2], Marianna Stamou[2], Karigowda J. Dammanahalli[3], Michael Duffel[3], Pamela J. Lein[2], and Hans-Joachim Lehmler[1]

[1]Department of Occupational and Environmental Health, College of Public Health, The University of Iowa, Iowa City, IA, USA, [2]Department of Molecular Biosciences, School of Veterinary Medicine, University of California, Davis, CA, USA, and [3]Department of Pharmaceutical Sciences and Experimental Therapeutics, College of Pharmacy, The University of Iowa, Iowa City, IA, USA

Abstract

1. Chiral polychlorinated biphenyls (PCBs) such as PCB 136 enantioselectively sensitize the ryanodine receptor (RyR). In light of recent evidence that PCBs cause developmental neurotoxicity via RyR-dependent mechanisms, this suggests that enantioselective PCB metabolism may influence the developmental neurotoxicity of chiral PCBs. However, enantioselective disposition of PCBs has not been fully characterized.
2. The effect of sex and cytochrome P450 (P450) enzyme induction on the enantioselective metabolism of PCB 136 was studied using liver tissue slices prepared from naïve control (CTL), phenobarbital (PB; CYP2B inducer) or dexamethasone (DEX; CYP3A inducer) pretreated adult Sprague-Dawley rats. PCB 136 metabolism was also examined in hippocampal slices derived from untreated rat pups.
3. In liver tissue slices, hydroxylated PCB (OH-PCB) profiles depended on sex and inducer pretreatment, and OH-PCB levels followed the rank orders male > female and PB > DEX > CTL. In contrast, the enantiomeric enrichment of PCB 136 and its metabolites was independent of sex and inducer pretreatment. Only small amounts of PCB 136 partitioned into hippocampal tissue slices and no OH-PCB metabolites were detected.
4. Our results suggest that enantioselective metabolism, sex and induction status of P450 enzymes in the liver may modulate the neurotoxic outcomes of developmental exposure to chiral PCBs.

Keywords

Atropisomeric enrichment, cytochrome P450 enzymes, sex differences

History

Received 4 February 2013
Revised 8 March 2013
Accepted 11 March 2013
Published online 12 April 2013

Introduction

Polychlorinated biphenyls (PCBs) are a class of persistent organic pollutants that were produced as complex mixtures by bulk chlorination of biphenyl. Although their commercial production in the United States was banned in the late 70s, PCBs are still present in the environment and released from sediments and soils (Hu et al., 2011) and oil-based pigments (Hu & Hornbuckle, 2010). Human exposure to PCBs occurs mainly via the diet, especially fish (Su et al., 2012), and inhalation of indoor and outdoor air (Hu et al., 2010). PCBs are classified as probably carcinogenic to humans by the International Agency for Research on Cancer, and exposure to PCBs has been linked to adverse effects on the immune system, the reproductive system and the endocrine system (USEPA, 2013). Epidemiological studies also demonstrate a link between developmental PCB exposures and adverse neurodevelopmental outcomes, including effects on attention, cognition, impulse control, memory, motor control and visual-spatial function (Dutta et al., 2012; Sagiv et al., 2012). Animal (Roegge et al., 2000; Widholm et al., 2001) and limited epidemiological data (Sagiv et al., 2012) suggest sex differences in PCB's neurodevelopmental effects.

Laboratory studies have implicated non-dioxin-like PCBs with multiple *ortho*-substitutions and the corresponding hydroxylated metabolites (OH-PCBs) as contributing to the adverse neurodevelopmental effects associated with developmental PCB exposures. Experimental data suggest that these effects are mediated by mechanisms independent of the aryl hydrocarbon receptor (Mariussen & Fonnum, 2006; Pessah et al., 2010), which is the cellular target of dioxin-like PCB congeners (van den Berg et al., 2006). Many of the most potent neurotoxic PCB congeners (Lehmler et al., 2005; Pessah et al., 2009) have 3–4 chlorine substituents in the *ortho*-position and display axial chirality, i.e. they exist as rotational isomers, or atropisomers, that are non-superimposable mirror images of each other. Chiral PCBs promote

Address for correspondence: Dr Hans-Joachim Lehmler, Department of Occupational and Environmental Health, The University of Iowa, University of Iowa Research Park, #221 IREH, Iowa City, IA 52242-5000, USA. Tel: (319) 335-4310. Fax: (319) 335-4290. E-mail: hans-joachim-lehmler@uiowa.edu

dendritic growth in hippocampal and cortical neurons by mechanisms involving ryanodine receptor (RyR) sensitization (Wayman et al., 2012b; Yang et al., 2009). The sensitization of RyR by chiral PCBs, such as PCB 136, is enantioselective, with only (−)-PCB 136 being active (Pessah et al., 2009). Since enantiomeric enrichment of chiral PCBs has been reported in environmental samples, wildlife, laboratory animals and humans (Lehmler et al., 2010), the enantiospecific effects of PCBs on RyR have significant human health implications.

The enantiomeric enrichment of PCBs in humans may be due to exposure to enantiomerically enriched PCBs through the food chain or enantioselective biotransformation to OH-PCBs in human tissues (Lehmler et al., 2010). Studies with rat CYP2B1 and human CYP2B6 enzymes (Warner et al., 2009) and hepatic microsomes (Wu et al., 2011) demonstrate that chiral PCBs are enantioselectively metabolized to OH-PCBs by P450 enzymes. Expression and activity of CYP2B1 displays sex specific differences (Asaoka et al., 2010) and is inducible by a range of xenobiotics (Meredith et al., 2003; Waxman & Walsh, 1982). Similarly, the human ortholog, CYP2B6, is a highly inducible enzyme that may display sex specific differences in expression and activities (Zanger et al., 2007). While there is some evidence that induction of P450 enzymes can alter PCB profiles in humans (Brown et al., 1989), little is known about the role of sex and P450 enzyme induction on enantioselective PCB metabolism. Furthermore, it is unknown if enantioselective PCB metabolism occurs only in the liver or also in target tissues of PCB toxicity, such as the hippocampus. Therefore, we investigated the sex-specific biotransformation of PCB 136 in rat liver slices prepared from naive animals and from animals pretreated to induce selected P450 enzymes. Because xenobiotics may be activated in different brain regions (Albores et al., 2001; Khokhar & Tyndale, 2012), we also examined PCB 136 metabolism in hippocampal tissue slices from uninduced animals. Our results demonstrate that PCB 136 is enantioselectively metabolized to OH-PCBs in the liver, that hepatic metabolism is influenced by sex and the inducer pretreatment, and that OH-PCBs were below the detection limit in hippocampal tissue slices.

Materials and methods

Reagents and materials

Dimethyl sulfoxide (DMSO), sodium chloride, potassium chloride, magnesium chloride, tetrabutylammonium sulfite and calcium chloride ($CaCl_2 \cdot 2H_2O$) were obtained from Fisher Scientific (Pittsburg, PA). Phenobarbital (PB), dexamethasone (DEX), sodium phosphate and sodium bicarbonate were purchased from Sigma-Aldrich Co. (St. Louis, MO). HEPES (4-(2-hydroxyethyl)-1-piperazineethanesulfonic acid) and glucose were from Research Products International Corp. (Drive Mount Prospect, IL). All reagents were used as received. Nanopure water (18 MΩ cm) was generated with a Milli-Q pore water system (Millipore, Billerica, MA). William's Medium E, Minimum Essential Medium (MEM) with Earle's salts and L-glutamine and heat inactivated horse serum were purchased from Invitrogen (Carlsbad, CA). (±)-PCB 136 was synthesized by the Ullmann coupling reaction (Shaikh et al., 2006). 2,2′,3,3′,6,6′-Hexachlorobiphenyl-4-ol (4-OH-PCB 136), 2,2′,3,3′,6,6′-hexachlorobiphenyl-5-ol (5-OH-PCB 136), 4,5-dimethoxy-2,2′,3,3′,6,6′-hexachlorobiphenyl (methylated derivative of 2,2′,3,3′,6,6′-hexachlorobiphenyl-4,5-diol (4,5-diOH-PCB 136)) and 2,2′,3′,4,6,6′-hexachloro-3-methoxybiphenyl were synthesized as described previously (Waller et al., 1999). Diazomethane was synthesized from N-methyl-N-nitroso-*p*-toluenesulfonamide (Diazald) using an Aldrich mini Diazald apparatus (Milwaukee, WI) (Black, 1982).

Liver slice preparation and culture procedure

Animals were treated according to protocols approved by the Institutional Animal Care and Use Committee. Female ($n = 9$) and male ($n = 8$) Sprague-Dawley rats (8-weeks-old) were obtained from Harlan Laboratories (Indianapolis, IN). The animals were housed in an animal facility approved by the Association for Assessment and Accreditation of Laboratory Animal Care with an alternating, reverse 12 h light, 12 h dark cycle with standard commercial food and tap water ad libitum. After a 1 week acclimation period, the rats were randomly separated into three treatment groups. One treatment group received intraperitoneal (i.p.) injections of PB (102 mg/kg b.w./d) in saline for three consecutive days. A second treatment group received i.p. injections of DEX (50 mg/kg b.w./day) in corn oil for four consecutive days (Kania-Korwel et al., 2008a; Thomas et al., 1983). These inducer treatments result in maximal induction of relevant P450 enzymes. Naïve animals were used as the control (CTL) group. Rats were euthanized 24 h after the last treatment by CO_2 asphyxiation followed by cervical dislocation. The liver was excised, immediately placed in cold Kreb-Henseleit (K-H) buffer (pH 7.5) and cut into lobes. The effects of PB or DEX treatment on body and liver weights are summarized in Table A1 (Appendix).

Tissue slices were prepared as described recently (Dammanahalli & Duffel, 2012; Fisher & Vickers, 2013). Briefly, cylindrical cores of 8 mm diameter were prepared using a coring tool. Liver slices (250 μm thick) were prepared with a Krumdieck tissue slicer (Alabama Research and Development Corporation, Munsford, AL). Tissue slices for gene expression analysis were cryopreserved in William's Medium E containing 12% DMSO. For metabolism experiments, two slices per incubation were immediately placed in glass scintillation vials with K-H buffer (2 mL). PCB 136 in DMSO (10 μL; final concentration of 5 μM) or DMSO alone (10 μL) was added and the slices were placed for 2 h in a dynamic incubation system at 37 °C under an atmosphere of 5% CO_2/95% air. The short, 2 h incubation time was chosen because P450 enzyme activities in tissue slices are known to decrease significantly after 4 h (Hashemi et al., 2000). Incubations were performed in triplicate per animal for PCB treatment groups and single incubation per animal for DMSO treatment group. At the end of the incubation, the slices were washed with cold K-H buffer (1 mL) and homogenized. Aliquots of tissue homogenates and medium (150 μL) were stored at −80 °C for lactate dehydrogenase (LDH) and protein determinations. Sodium hydroxide (0.5 M, 2 mL) was added to the remaining medium and tissue homogenate samples and

the samples were stored at −20 °C prior to PCB and metabolite extraction.

Detection of liver slice viability

The viability of the liver slices was assessed by measuring the percentage of LDH released into medium using the Cytotoxicity Detection Kit PLUS following the instructions of the manufacturer (Roche Applied Sciences, Indianapolis, IN). LDH release was expressed as percentage of total enzyme using the formula: LDH release $= A_1 \times D_1/(A_1 \times D_1 + A_2 \times D_2)$, where A_1 and A_2 are the absorbance of the medium and homogenate samples, respectively; D_1 and D_2 are the dilution factors for medium and homogenate samples, respectively (Valentovic et al., 1995).

Hippocampal tissue slice preparation and culture procedure

All procedures and protocols involving animals for the preparation of hippocampal tissue slices were performed according to protocols approved by the Institutional Animal Care and Use Committee of the University of California, Davis. Timed-pregnant Sprague Dawley rats purchased from Charles River Laboratories (Hollister, CA) were housed individually in standard plastic cages with corn cob bedding in a temperature controlled room (22 ± 2 °C) on a 12 h reverse light dark cycle. Food and water were provided *ad libitum*. Pups were euthanized on postnatal day 4 (PND4) by decapitation prior to harvesting of hippocampi for culture.

The sex of each pup was initially determined by anogenital distance and confirmed by inspection of internal organs (Liu et al., 2008). Hippocampal slice cultures were prepared as previously described (Lein et al., 2011). Briefly, 400 µm thick hippocampal slices were cut using a McIIwain tissue chopper (Brinkman, Westbury, NY) and transferred onto 0.4 µm Millicell cell culture inserts (Millipore, Billerica, MA) in six-well culture plates ($n = 6$ slices per well) and maintained in MEM with Earle's salts and L-glutamine supplemented with 20% heat-inactivated horse serum, 1 mM $CaCl_2$, 2 mM $MgSO_4$, 1 mg/L insulin, 1 mM $NaHCO_3$, 0.5 mM L ascorbate, 30 mM HEPES and 2.3 g/L D-glucose at pH 7.3.

Racemic PCB 136 or vehicle (0.1% DMSO) was added to 1 mL of culture medium in each well beginning on day 5 *in vitro* (DIV). Medium (supplemented with PCB 136 or vehicle as appropriate) was replaced every 2 d for 14 d. Conditioned medium removed at each time point was collected in glass tubes with Teflon lined screw caps and stored at −20 °C until analyzed. After 14 d of PCB exposure, hippocampal slices were collected in glass tubes with Teflon lined screw caps and stored at −20 °C until analyzed.

Viability assessments of hippocampal slice cultures

Viability was assessed by LDH release using the CytoTox-ONE™ Homogenous Membrane Integrity Assay (Promega, Madison, WI) as per the manufacturer's directions. Propidium iodide (PI) (2 µM) from Molecular Probes (Eugene, OR) in DMSO was used as a fluorescent indicator of cytotoxicity in a separate set of hippocampal slice cultures. Slices were incubated with PI for 1 h, then transferred to new plates for imaging both before (5 DIV) and after (8 DIV) PCB 136 treatment.

Total RNA extraction and reverse transcription

For liver, total RNA was extracted from one tissue slice cryopreserved in 12% DMSO in William's Medium E per rat using the Qiagen RNeasy Mini Kit (Germantown, MD) according to the manufacturer's instructions. For brain, total RNA was extracted from hippocampal slice cultures derived from PND4 rat pups using Trizol reagent (Invitrogen, Carlsbad, CA) according to the manufacturer's instructions. Following digestion of total RNA samples with 100U of DNase I (Invitrogen) to remove possible genomic DNA contamination, 1 µg of total RNA per sample was reverse transcribed to cDNA with 200U of Superscript III reverse transcriptase using the Invitrogen Superscript III First Strand Synthesis kit with 50 ng/µL of random hexamer primers, according to the manufacturer's protocol. The OD_{260nm}/OD_{280nm} for cDNA samples was confirmed to be >1.8.

Quantitative real time polymerase chain reaction assays

Primer (forward and reverse primers) and probe sets specific for each P450 isoform were designed using PrimerBlast from NCBI (Bethesda, MD) and PrimerQuest software (IDT, Coralville, IA) (Table A2). Specificity of the primers and probes for each gene was confirmed by BLAST searches conducted against nucleotide collection databases for *Rattus Norvegicus*. To avoid genomic DNA amplification, primers were designed to span an exon–exon junction (whenever this information was available for the particular gene). The absence of dimers and hairpins for both primers and probe was confirmed for all gene assays using OligoAnalyzer software from IDT. P450 isoform specific primer and probe sets were synthesized by IDT, which was also the source of a commercially available primer and probe set for the reference gene (phosphoglycerate kinase 1; Pgk1) (Nelissen et al., 2010). Amplicons were between 90 and 200 nucleotides long. No-template and no-enzyme controls were run with each assay and confirmed by quantitative polymerase chain reaction (qPCR) analyses to produce negligible signal (usually >39 Ct value). All fluorescent probes contained a ZEN internal quencher (IDT) for elimination of background fluorescence. Specificity of the CYP-specific primer sets was confirmed by agarose gel electrophoresis of RT-PCR amplification products from total RNA extracted from homogenized rat liver tissue.

qPCR was performed on a 7500 Fast Real-Time PCR System (Applied Biosystems, Foster City, CA) using the Taqman Universal PCR Master Mix (Life Sciences, Grand Island, NY). Amplification was performed according to the manufacturer's instructions. Thermal cycling conditions comprised an initial annealing step at 50 °C for 2 min, followed by a denaturation step at 95 °C for 10 min and 40 cycles at 95 °C for 15 s and 60 °C for 1 min.

Analysis of amplification results was performed using the 7500 Fast System SDS software (Applied Biosystems) to obtain Ct values (Pfaffl et al., 2002). For all samples, Ct value for the P450 transcript was normalized on the basis of

the reference gene content to account for any differences in the precise amount of total RNA present in each sample, potential sample degradation, and/or differences in sample loading.

To determine the fold change in expression of specific P450 isoform transcripts following induction by PB or DEX, relative transcript expression between control and treated animals was calculated using the REST2009 software (Qiagen) as determined by the following formula: $R = (E_{target})^{\Delta Ct(control-sample)}_{target} / (E_{ref})^{\Delta Ct(control-sample)}_{ref}$ (Pfaffl, 2001), where R refers to the fold change in expression of the target gene in treated versus control samples normalized to the reference gene; E_{target} refers to qPCR efficiency of amplifying the target gene; E_{ref} refers to the qPCR efficiency of amplifying the reference gene; Ct refers to the amplification cycle when fluorescence exceeds a manually defined threshold. Efficiency for each gene was calculated from the dilution curve for that particular gene using the formula $E = 10^{[-1/slope]}$ (Pfaffl, 2001). The ΔCt value for each gene was determined by subtracting the average Ct value (duplicate) of the respective gene in the control from the average Ct value (duplicate) of the same gene in the sample. The REST2009 software determines the statistical significance of calculated expression ratios using randomization algorithms (random pairing of controls and samples from the gene of interest and the reference gene and calculation of their expression ratio). Efficiencies were checked for all genes and ranged between 0.88 and 1.16. Ratios were determined for P450 genes with average Ct values at all dilution points lower than 37. Target genes were considered undetected (not quantifiable or unexpressed) when the Ct value was above 37.

Extraction of PCB 136 and its metabolites

PCB 136 and its metabolites were extracted from the tissue homogenates and medium samples using a previously reported liquid–liquid extraction procedure (Wu et al., 2011). In short, all samples were spiked with appropriate surrogate standards for PCBs (2,3,4,4′,5,6-hexachlorobiphenyl, 250 ng) and OH-PCBs (4-OH-2′,3,3′,4,5,5′-hexachlorobiphenyl, 200 ng) at the beginning of the extraction. For the brain tissue slices, 2,3,5,6-tetrachlorobiphenyl (500 ng) was added as PCB surrogate standard. The medium and homogenate samples were acidified with 6 M hydrogen chloride (1 mL) and extracted with 2-propanol (3 mL) and hexane-MTBE (1:1, v/v; 5 mL). The organic phase was washed with 1% KCl (2 mL). After derivatization with diazomethane, the samples were spiked with the internal standard (2,2′,3,4,4′,5,6,6′-octachlorobiphenyl, 200 ng). The samples were further cleaned by shaking the sample with 2-propanol (2 mL) and tetrabutylammonium sulfite (2 mL), and reshaking after adding nanopure water (5 mL). The organic extract was mixed with concentrated sulfuric acid (2 mL), kept overnight and transferred to vials.

Analysis of PCB 136 and its metabolites

The levels of PCB 136 and its hydroxylated metabolites (as methoxylated PCB derivatives) in liver and brain samples were determined simultaneously using an Agilent 6980N gas chromatograph (GC) equipped with a ^{63}Ni micro-electron capture detector (μ-ECD) and a DB1-MS capillary column (60 m × 0.25 mm inner diameter (ID) × 0.25 μm film thickness; Agilent, Santa Clara, CA) (Kania-Korwel et al., 2012). The injector and detector temperatures were 280 °C and 300 °C, respectively. The temperature program was as follows: 100 °C for 1 min, 5 °C/min to 250 °C, hold for 20 min, 5 °C/min to 280 °C, hold for 3 min. The flow rate was 1 mL/min. The concentrations of PCB 136 and its hydroxylated metabolites were within the linear range of calibration curves (1 to 1000 ng/mL) in all samples. Detailed information about detection limits are shown in Table A3. The recoveries of PCB 65, PCB 166 and 4-OH-PCB 159 were 92 ± 8%, 86 ± 12% and 87 ± 15%, respectively. The levels of PCB 136 and its hydroxylated metabolites in liver slices were adjusted for recoveries. Protein levels were determined with the method of Lowry using bovine serum albumin as standard (Lowry et al., 1951).

Enantioselective analysis of PCB 136 and OH-PCB 136 atropisomers

Atropisomers of PCB 136 and 5-OH-PCB 136 were separated on the same instrument described above using a Chirasil-Dex capillary column (25 m × 0.25 mm ID × 0.25 μM film thickness; Agilent, Santa Clara, CA) (Wu et al., 2011). The injector and detector temperatures were kept at 250 °C. The flow rate was 3 mL/min. The temperature program was as follows: 15 °C/min from 50 to 135 °C, hold for 800 min, 15 °C/min to 200 °C, hold for 10 min. 4-OH-PCB 136 atropisomers were separated with a Cyclosil-B capillary column (30 m × 0.25 mm ID × 0.25 μm film thickness; Agilent, Santa Clara, CA) (Kania-Korwel et al., 2011; Wu et al., 2011). The temperature program was as follows: 15 °C/min from 50 to 160 °C, hold for 360 min, 15 °C/min to 200 °C, hold for 10 min. The enantiomeric fraction (EF) values for PCB 136, 4-OH and 5-OH-PCB 136 were determined as EF = Area $E_{(2)}$/(Area $E_{(1)}$ + Area $E_{(2)}$). Additional details about detection limits and resolution of PCB and OH-PCB atropisomers are provided in Table A4.

Statistics

GraphPad Prism 4 (version 4, GraphPad Software, La Jolla, CA) or SAS software (version 9.3, SAS Institute, Cary, NC) were used for the statistical analysis. All data are presented as the mean ± standard deviation/standard error of mean (as indicated in the table or figure legends). One-way or two-way analysis of variance (ANOVA) were used to identify significant differences in animal body weight, liver weights, tissue slice viability, gene expression, PCB and OH-PCB levels, and EF values as appropriate (see text and figure legends for additional details). $p < 0.05$ indicated statistically significant differences.

Results

Viability of liver tissue slices

Adult animals were used as the source of liver slices for studies of PCB metabolism for several reasons: first, yield and viability of liver tissue slices are significantly greater for slices prepared from adult versus neonatal rodents. Second,

maternal PCB and OH-PCB levels are likely a good surrogate for fetal and neonatal PCB and OH-PCB profiles and EF values since PCBs and OH-PCBs can cross the placenta (Meerts et al., 2002; Park et al., 2008) and are transferred to the offspring via the breast milk (Inoue et al., 2006). In addition, activities of P450 isoforms involved in PCB metabolism do not display marked age dependencies in rats after weaning (Waxman et al., 1985). Therefore, it is unlikely that PCB metabolism by liver slices prepared from post-weaning rats display a marked age dependence; however, this does not preclude differences in PCB metabolism between neonatal and adult liver and this possibility should be investigated in future studies.

LDH release was assessed to determine the effects of a 2 h incubation with PCB 136 (5 μM) on the viability of liver tissue slices prepared from adult CTL animals or adult rats pretreated with PB or DEX. All slices used in the PCB 136 metabolism experiments were viable (i.e. LDH release <30%), as indicated by a LDH release of only $13.2 \pm 6.6\%$ to the medium over the 2 h incubation time (Naik et al., 2004; Valentovic et al., 1995). The viability of liver tissue slices from DEX pretreated male and female rats ($10.4 \pm 3.6\%$ and $19.6 \pm 10.4\%$ LDH release, respectively) was within the acceptable range, which suggests that the general toxicity caused in the DEX-treated animals did not adversely affect tissue slice viability. There was no significant difference in LDH release between slices treated with PCB 136 or DMSO (vehicle) alone ($13.1 \pm 6.6\%$ versus $13.6 \pm 6.8\%$, respectively), which suggests that a 2 h incubation with PCB 136 at 5 μM was not acutely toxic to the liver slices.

Viability of hippocampal tissue slices

Rat pups at PND4 were used as the source of hippocampal slice cultures because this age is optimal for this preparation (Lein et al., 2011), and because the developing brain is the principal target in PCB neurotoxicity. Based on viability assays of cultures exposed to varying concentrations of racemic PCB 136 for 3 d, separate cultures were set up to examine whether viability was altered by exposure to PCB 136 at 5 μM for 14 d. Confocal microscopy images of PI uptake indicated no significant differences between control slice cultures exposed to vehicle for 14 d versus slice cultures exposed to PCB 136 at 5 μM for 14 d (data not shown). Quantitative image analyses of PI uptake immediately prior to and after a 3 d exposure to PCB 136 suggest an increase in PI uptake in slices exposed to PCB 136 at concentrations of 10 μM, but quantitative analysis of PI fluorescence indicated that this apparent increase was not statistically significant relative to slices incubated in vehicle only (Figure 1A and B). Subsequent subacute exposure experiments investigating the effect of PCB 136 on LDH release showed that LDH release in slice cultures treated for 14 days at concentrations $\leq$5 μM PCB 136 was not significantly different than vehicle controls (Figure 1C).

P450 gene expression in liver tissue slices obtained from adult rats

Transcript levels of cytochrome P450 enzymes involved in the metabolism of PCB were determined in cryopreserved liver tissue slices to document the induction of these enzymes by PB and DEX relative to CTL animals at the time of tissue slice preparation (Figures 2 and 3).

Female rat liver

CYP2B1/2 was significantly upregulated in tissue slices from both PB and DEX-treated female rats compared to female CTL rats, with a rank order of PB > DEX (Figure 2). Transcript levels of CYP3A2 and CYP1A2 (data not shown) in tissue slices from female rats were not significantly changed due to PB or DEX treatment. Similar to male rats, CYP4X1 and CYP2S1 gene expression was not detected in liver tissue slices from female rats from any treatment group (data not shown).

Male rat liver

In liver slices from male rats, CYP2B1/2 was significantly upregulated by PB compared to CTL animals. A slight increase was noted with DEX treatment; however, this effect was not statistically significant (Figure 2). Compared to CTL males, CYP3A2 was significantly induced by DEX but not PB treatment. Transcript levels of CYP1A2 in tissue slices were not changed by PB or DEX treatment (data not shown). CYP4X1 and CYP2S1 transcripts were not detected in liver tissue slices from male rats from any treatment group (data not shown).

Male versus female rat liver

In addition to differences in P450 enzyme transcript levels between treatment groups, there were also statistically significant differences in the gene expression of P450 enzymes between male and female rats (Figure 3). Transcript levels of CYP2B1/2 and CYP3A2 genes were lower in tissue slices from female compared to male rats from both the CTL and PB treatment groups, whereas CYP1A2 gene expression was comparable between both sexes in both treatment groups. In the DEX treatment group, CYP3A2 expression was also lower in slices from female compared to male animals. Transcript levels of the CYP2B1/2 gene were comparable in the DEX treatment group, whereas CYP1A2 expression was higher in tissue slices from female compared to male rats.

P450 gene expression in hippocampal tissue slices from neonatal rats

The mRNA levels of CYP2B1/2, CYP3A2, CYP1A2, CYP4X1 and CYP2S1 were determined in untreated tissue slices from hippocampi harvested on PND4. Transcripts of CYP2B1/2, CYP3A2, CYP1A2, CYP4X1 and CYP2S1 genes were detected in hippocampal slice cultures, and levels of these mRNA did not change significantly as a function of DIV (Figure A1).

PCB 136 levels in liver tissue slices relative to medium

Liver tissue slices were prepared from adult female and male rats and exposed for 2 h to racemic PCB 136 (5 μM). Medium-to-tissue slice ratios (Figure 4) and protein adjusted PCB 136 levels (Table A5) were calculated to determine PCB136 uptake and accumulation in tissue slices.

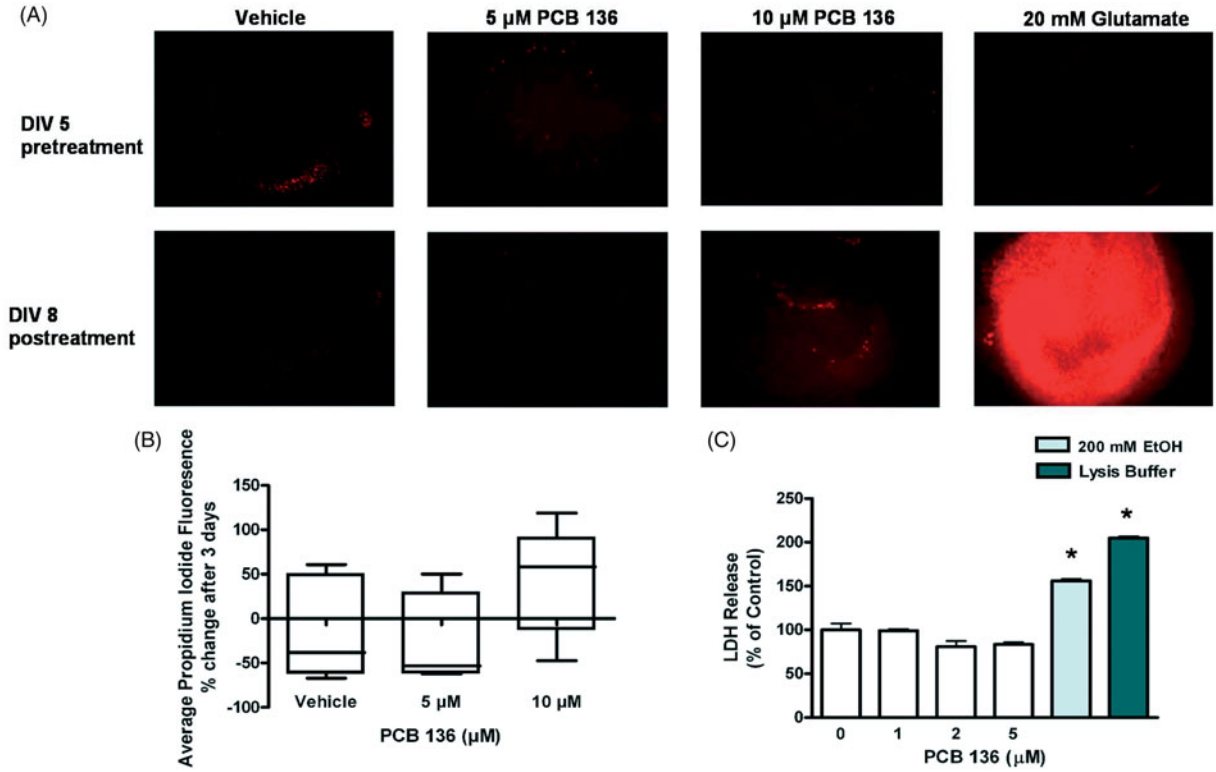

Figure 1. Effects of PCB 136 on cell viability in hippocampal slice cultures. Hippocampal slices cultured from postnatal day 4 rats were exposed to racemic PCB 136 added to the culture medium for 3 d beginning at 5 DIV. (A) Representative confocal photomicrographs of PI uptake immediately prior to (top panels) and after a 3 d exposure to vehicle (0.1% DMSO), glutamate (20 mM, used as a positive control) or varying concentrations of racemic PCB 136 (bottom panels). Bar = 100 μm. (B) Quantification of PI fluorescence in each hippocampal slice. Fluorescence prior to exposure was subtracted from fluorescence levels after the treatment period to assess changes in PI uptake as a function of treatment. While glutamate significantly increased PI uptake, PCB 136 at 5 or 10 μM had no significant effect on PI uptake (one-way ANOVA). Data expressed as the mean ± SEM ($n = 5$ wells per treatment group). (C) Effects of PCB 136 on cellular membrane integrity in hippocampal slice as determined by release of LDH. Hippocampal slices were exposed to vehicle or varying concentrations of racemic PCB 136 added to the culture medium every other day for 14 d beginning at 5 DIV. Exposure to PCB 136 for 14 d at ≤5 μM did not significantly alter LDH release relative to vehicle controls. In contrast, a 14 d exposure to ethanol (200 mM) or treatment with lysis buffer immediately prior to collection of medium for LDH analysis significantly increased LDH release. Data expressed as the mean ± SEM ($n = 2$ wells per treatment group). *Significantly different from control at $p < 0.001$ (one way ANOVA with *post-hoc* Tukey's test).

Female liver tissue slices

At 0 min, only traces of PCB 136 were associated with tissue slices prepared from female rats. After 2 h, the levels of PCB 136 in medium were still higher compared to tissue slice levels; however, a considerable amount of PCB 136 had partitioned into the tissue slices, as indicated by medium to slice ratios ranging from 3.2 to 4.1 for the different tissue slice incubations (Figure 4A). Levels of PCB 136 ranged from 42 to 53 ng/mg protein in tissue slices, which corresponds to 21–25% of the total PCB 136 dose added to each incubation (Table A5). No clear effect of inducer pretreatment on PCB levels in the tissue slices was observed.

Male liver tissue slices

As with tissue slices from female rats, PCB 136 had partitioned into the liver slices prepared from male rats after 2 h incubation, with medium to slice ratios of PCB 136 ranging from 2.8 to 7.3 for the different tissue slice incubations (Figure 4B). The highest medium to tissue slice ratio was observed for tissue slices from PB pretreated male animals. This ratio was significantly higher from the ratio observed for tissue slices from female, PB pretreated rats due to significantly lower PCB levels in the tissue slices. PCB 136 levels in tissue slices were 21 to 33 ng/mg protein. The levels correspond to 13–23% of the total PCB 136 dose (Table A5). Overall, less PCB 136 was detected in tissue slices from male versus female rats. Consistent with observations in liver slices from female rats, inducer pretreatment had no effect on PCB levels in liver slices prepared from male rats (Table A5).

PCB 136 levels in hippocampal tissue slices relative to medium

Hippocampal tissue slices were prepared from both female and male pups at PND4 and incubated for 14 d with racemic PCB 136 (5 μM). Because P450 enzyme activities in brain tissue are lower compared to the liver, a comparatively long incubation time was selected to maximize the metabolite formation and, thus, allow their detection in culture medium and tissue slices. The amount of PCB 136 was measured in medium collected every other day and in tissue slices at the end of the experiment.

Hippocampal slice cultures from female pups

In hippocampal slice cultures from female pups, the average PCB 136 concentration in the incubation medium was 830 ± 80 ng/mL. Based on these actual medium

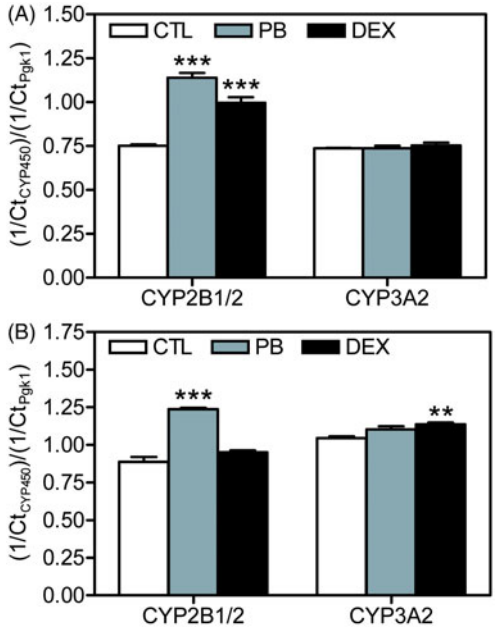

Figure 2. Effects of PB and DEX treatment on hepatic cytochrome P450 transcript levels in rat liver slices prepared from (A) female and (B) male rats. Total RNA was isolated from liver slices obtained from adult female and male rats (CTL or treated with PB or DEX), and reverse transcribed to cDNA. Transcript levels of specific cytochrome P450 isoforms was determined by qPCR. The relative amount of transcript is expressed as the Ct value for a specific CYP normalized to the Ct value for the reference gene (Pgk1) in the same sample. Data are expressed as the mean ± S.E.M. ($n = 2$–3 rats per treatment; see Table S1). $^{**}p < 0.01$; $^{***}p < 0.001$ indicates statistically significant differences between treated and untreated rats as determined by two-way ANOVA (GraphPad Prism software).

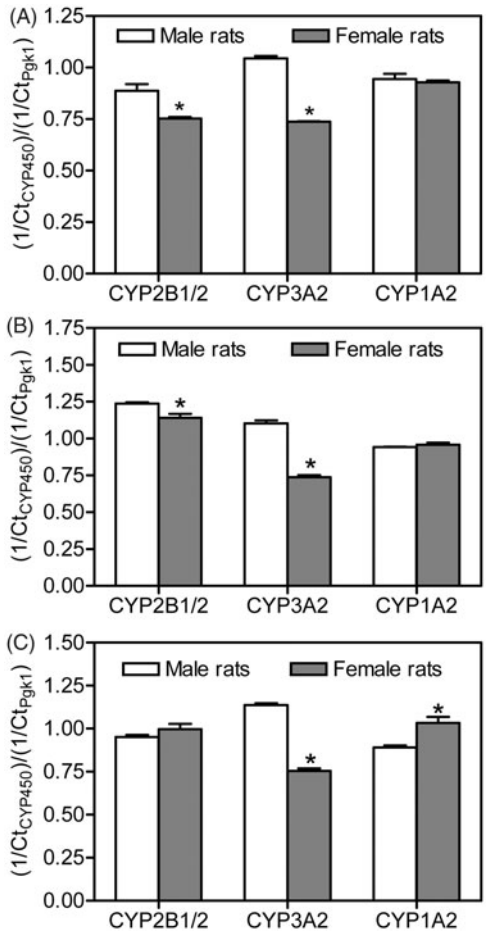

Figure 3. Sex differences in hepatic cytochrome P450 transcript levels in rat liver slices prepared from (A) CTL, (B) PB- and (C) DEX-treated rats. Total RNA was isolated from liver slices obtained from adult female and male rats (CTL or treated with PB or DEX), reverse transcribed to cDNA, and transcript levels of specific cytochrome P450 isoforms were determined by qPCR. The relative amount of transcript is expressed as the Ct value for a specific cytochrome P450 gene normalized to the Ct value for the reference gene (Pgk1) in the same sample. Data are expressed as the mean ± S.E.M. ($n = 2$–3 rats per treatment; see Table S1). $^{*}p < 0.05$ indicates statistically significant differences between the sexes as determined by two-way ANOVA (GraphPad Prism software).

concentrations, the total dose was 5.8 µg PCB 136 per incubation (theoretical dose: 12.6 µg PCB 136). The average PCB 136 amount associated with the tissue slices was 27 ± 15 ng, which corresponds to 0.2% of the total PCB dose added to the incubations or 1.5 ± 0.8% of the PCB 136 (1.8 µg PCB 136) added on day 12. The corresponding medium-to-tissue slice ratio of PCB 136 was 24 ± 8 on day 14 (Figure 4).

Hippocampal slice cultures from male pups

In hippocampal slice cultures from male pups, the average PCB 136 levels in the incubation medium was 570 ± 220 ng/mL. The corresponding total dose was 4.0 µg PCB 136 per incubation (theoretical dose: 12.6 µg PCB 136). The PCB 136 amount associated with tissue slices was 32 ± 6 ng. This corresponds to 0.3% of the total PCB dose in each incubation and 1.8 ± 0.3% of the PCB 136 (1.8 µg PCB 136) added on day 12. The medium-to-tissue slice ratio of PCB 136 was 26 ± 10 on day 14 (Figure 4). Overall, PCB 136 levels were comparable between hippocampal tissue slices from male versus female rats.

Hydroxylated PCB 136 metabolites in liver slices

Female liver slices

In liver slices from female rats, ≤5% of the total PCB 136 was metabolized to OH-PCBs within 2 h. The sum of the OH-PCBs (ΣOH-PCBs) and 5-OH-PCB 136 levels in the tissue slices increased in the order PB > DEX > CTL (Table A6). Specifically, 0.5 nmol and 0.3 nmol of ΣOH-PCBs were detected in liver slices from PB- and DEX-treated female rats, whereas less ΣOH-PCBs (0.05 nmol) were detected in liver slices from female CTL rats. 4-OH-PCB 136 levels were essentially constant for the different tissue slice preparations. While the metabolite profile in liver slices prepared from female PB- and DEX-treated rats followed the rank order 5-OH-PCB 136 >> 4-OH-PCB 136 > 4,5-diOH-PCB 136 (Figure 5A), 4-OH-PCB 136 was the major metabolite in liver slices obtained from female CTL rats, with 4-OH-PCB 136 levels approximately three times higher than 5-OH-PCB 136 levels. No OH-PCBs were released from the tissue slices into the incubation medium.

Male liver slices

Similar to female rats, the ΣOH-PCBs increased in the order PB > DEX > CTL in experiments using tissue slices from male rats, with at least 11% of the total PCB being converted

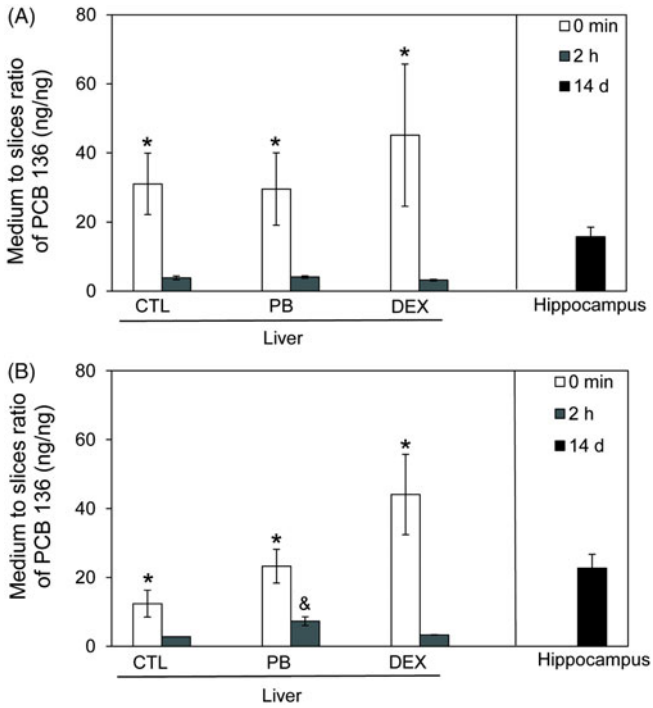

Figure 4. Partitioning of PCB 136 from medium into liver tissue slices prepared from (A) female and (B) male adult rats and hippocampal tissue slices obtained from neonatal rats. In liver tissue slices from CTL rats and PB or DEX pretreated rats, the medium to slice ratio of PCB 136 significantly decreased between 0 min and 2 h, with the PCB 136 level in medium being only 3–7-times higher compared to tissue slice levels after a 2 h incubation. In hippocampal tissue slices from neonatal rats, some PCB 136 was detected in the tissue slices; however, most of the PCB 136 added to the cultures was still present in medium. Data are presented as the mean ± S.E.M. ($n = 2$ or 3, with triplicate incubations; see also Table S1). * $p < 0.05$ indicates significant differences between 0 h and 2 h medium to tissue ratios; $^{\$}p < 0.05$ indicates significantly higher medium to tissue ratios in incubations with tissue slices from male compared to female rats as determined by two-way ANOVA (SAS software).

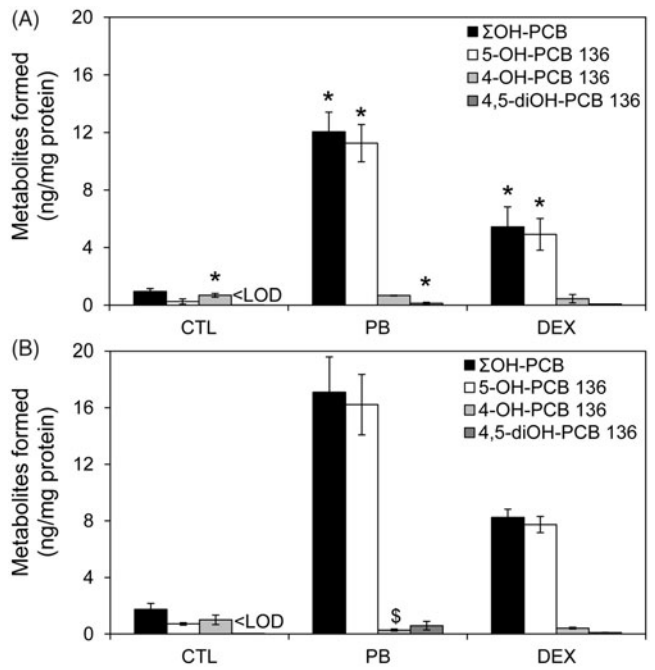

Figure 5. Quantification of PCB 136 metabolites in liver tissue slices from (A) female and (B) male rats. PCB 136 is metabolized by P450 enzymes to 4-OH-PCB 136, 5-OH-PCB 136 and 4,5-diOH-PCB 136. PCB 136 metabolites formed in liver tissue slices from PB- and DEX-treated rats followed the rank order: 4-OH-PCB 136 ~ 4,5-diOH- PCB 136<< 5-OH-PCB 136. While female and male rats typically displayed a similar metabolite pattern, metabolite levels were typically lower in female rats compared to male rats. Data are presented as the mean ± standard deviation ($n = 2$ or 3, with triplicate incubations; see also Table S1). *$p < 0.05$ indicates significantly lower OH-PCB levels in tissue slices prepared from female than male rats; $^{\$}p < 0.01$ indicates significantly higher 4-OH-PCB 136 levels in tissue slices prepared from female than male rats as determined by two-way ANOVA (SAS software).

to OH-PCBs (Table A6). OH-PCBs accounting for approximately 15% of ΣOH-PCBs were also detected in the medium of liver slice incubations from PB- and DEX treated male animals. The ΣOH-PCBs and 5-OH-PCB 136 levels in liver slices followed the rank order PB > DEX > CTL. Levels of 4-OH-PCB 136 in the tissue slices seemed to decrease in the order PB < DEX < CTL. Furthermore, the OH-PCB levels (including ΣOH-PCB) in liver slices from male rats were generally higher compared to liver slices from female rats from the same treatment group (Figure 5A versus B).

The metabolite profile in liver slices from DEX-treated male animals followed the rank order 5-OH-PCB 136 >> 4-OH-PCB 136 > 4,5-diOH-PCB 136 (Figure 5B) and, thus, was comparable to the profile observed in female PB- and DEX-treated rats (Figure 5A). In contrast, the metabolite profile in liver slices from PB-treated male rats displayed a rank order of 5-OH-PCB 136 >> 4,5-diOH-PCB 136 > 4-OH-PCB 136, which is different from incubations using liver slices from PB- and DEX-treated female and DEX-treated male rats. Similar to experiments using liver slices from female CTL rats, 4-OH-PCB was the major metabolite in incubations with liver slices from male CTL rats, with a rank order of 4-OH-PCB 136 > 5-OH-PCB 136. 4,5-diOH-PCB 136 was below the detection limit in tissue slices from CTL rats.

Hydroxylated PCB 136 metabolites in hippocampal tissue slices

No OH-PCBs were detected in the hippocampal tissue slices obtained from female or male pups or in the incubation medium. This observation suggests that levels of OH-PCBs are below or equal to the background level observed in vehicle treated hippocampal slice cultures (i.e. approximately 0.4, 1.4 or 0.1 ng/mg for 5-OH-PCB136, 4-OH-PCB136 or 4,5-diOH-PCB 136, respectively; Table A3).

Enantiomeric enrichment of PCB 136 and OH-PCB 136 in liver slices from female and male rats

The enantiomeric enrichment of PCB 136, 5-OH-PCB 136 and 4-OH-PCB 136 was only investigated in incubations with liver slices from PB- and DEX-treated animals due to the low metabolite levels observed for incubations with liver slices from CTL rats (Table A4). Figure 6 shows representative chromatograms of racemic 5-OH-PCB 136 and 4-OH-PCB 136 standards and the selective enrichment of both hydroxylated metabolites in liver slices from PB- and DEX-treated female and male rats after incubation with racemic PCB 136. (−)-PCB 136 was slightly enriched in liver slices prepared from PB- and DEX-treated male and female rats (Figure 7). The EF values in the different treatment groups ranged from 0.45 to 0.47 and no statistically significant differences

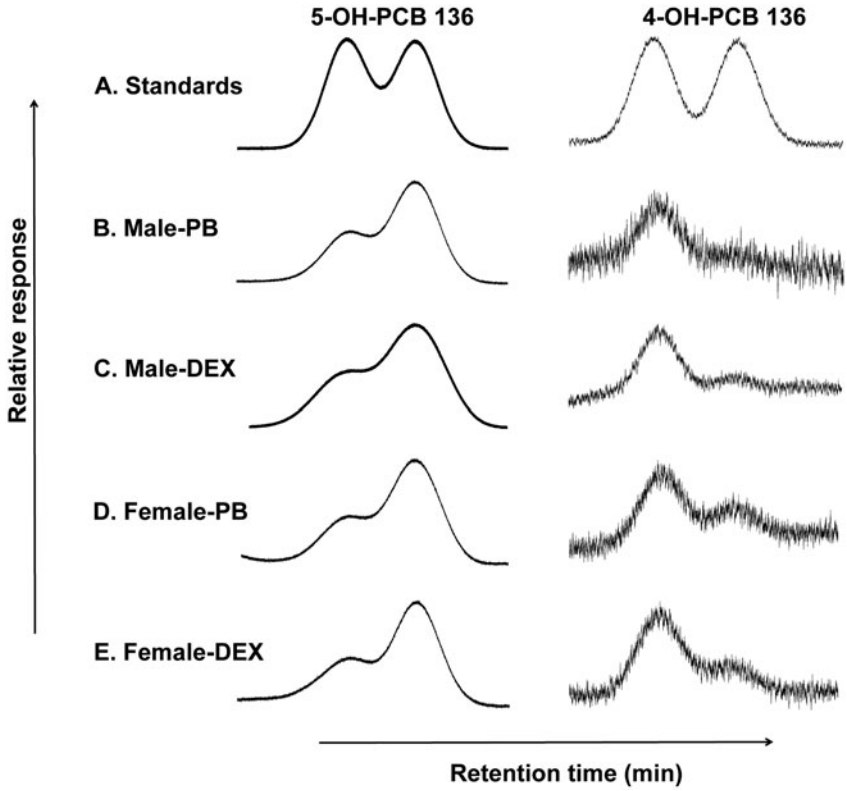

Figure 6. The second eluting atropisomer of 5-OH-PCB 136 ($E_{(2)}$-5-OH-PCB 136) and the first eluting atropisomer of 4-OH-PCB 136 ($E_{(1)}$-4-OH-PCB) are formed enantioselectively in liver tissue slices prepared from PB- or DEX-treated rats incubated with PCB 136. Representative chromatograms of racemic 5-OH-PCB 136 and 4-OH-PCB 136 standards (A) and liver slices incubated with PCB 136 (5 μM, 2 h) that were prepared from: (B) Male PB-treated rats; (C) male DEX-treated rats, (D) female PB-treated rats and (E) female DEX-treated rats. Atropisomers of 5-OH-PCB 136 and 4-OH-PCB 136 were separated as their methylated derivatives on Chirasil-Dex and Cyclosil-B columns, respectively.

between sex or inducer treatment were observed. The second eluting atropisomer of 5-OH-PCB 136 ($E_{(2)}$-5-OH-PCB), which is formed from (+)-PCB 136 (Wu et al., 2011), was enriched to a similar extent in tissue slices prepared from male and female rats, irrespective of the inducer treatment (EF = 0.69–0.74) (Figures 6 and 7). At the same time, the first eluting atropisomer of 4-OH-PCB 136 ($E_{(1)}$-4-OH-PCB), which is a metabolite of (−)-PCB 136 (Wu et al., 2011), was enriched in the tissue slices (Figures 6 and 7). The EF values of 4-OH-PCB 136 ranged from 0.22 to 0.36, with incubations employing liver slices from male rats displaying a more pronounced enantiomeric enrichment compared to incubations using liver slices from female rats. As with the parent PCB, no significant differences in the EF values were observed between sex or inducer treatment for both OH-PCB metabolites.

Discussion

PCB 136 is a RyR active PCB congener (Pessah et al., 2006) of environmental relevance (Lehmler et al., 2010) that is oxidized enantioselectively by P450 enzymes to hydroxylated metabolites (Schnellmann et al., 1983; Waller et al., 1999; Wu et al., 2011). The hydroxylated metabolites are potent sensitizers of RyRs (Pessah et al., 2006) and, thus, may play a role in the developmental neurotoxicity of PCBs (Wayman et al., 2012b). The present study employs liver slice cultures to study the role of sex and hepatic P450 enzyme induction in the enantioselective oxidation of neurotoxic PCB congeners. Tissue slices were employed as an *in vitro* system that, in contrast to recombinant enzymes or subcellular fractions, reflects the complex metabolic processes that may contribute to sex-specific PCB metabolism in the liver (Ioannides, 2013; Lake & Price, 2013; Ohyama et al., 2005a,b).

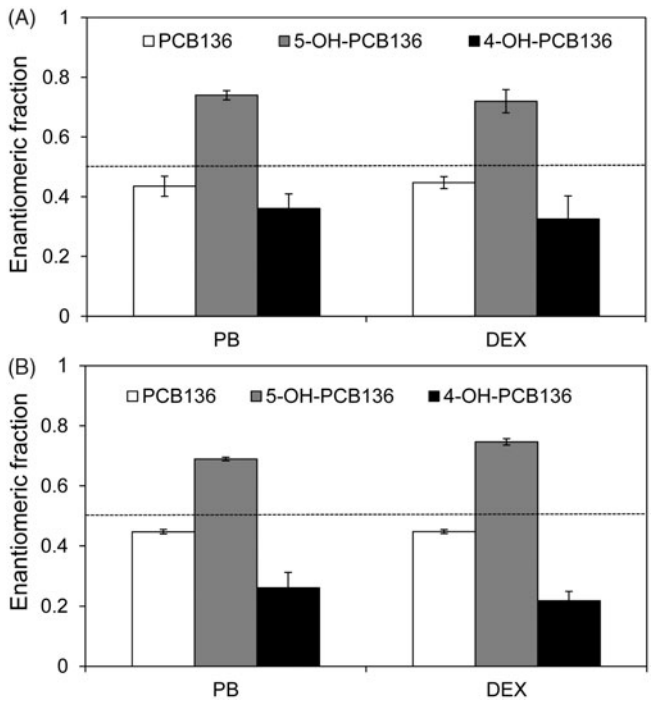

Figure 7. Enantiomeric enrichment of PCB 136 and its hydroxylated metabolites in rat liver tissue slices from (A) female and (B) male rats. The EF of PCB 136 in liver slices from PB- or DEX-treated rats showed a slight enrichment of (−)-PCB 136. The second eluting atropisomer of 5-OH-PCB 136, which is formed from (+)-PCB 136, was enriched. In contrast, the first eluting atropisomer of 4-OH-PCB 136, which is a metabolite of (−)-PCB 136, was enriched. No statistically significant differences in EF values between treatment groups or sexes were observed by ANOVA with Tukey multiple comparisons (SAS software). Data are presented as the mean ± SD ($n = 3$). The dotted line represents the EF value of the racemic PCB 136 in which the liver slices were incubated (0.498 ± 0.005; $n = 12$).

Furthermore, liver tissue slices can be prepared from animals pretreated with inducers of P450 enzymes (Hashemi et al., 2000), thus modeling the effect of the induction of hepatic P450 enzymes by xenobiotics on the disposition of PCBs in laboratory animals and humans (Reed et al., 2001; Ulrich et al., 2001). Like other *in vitro* systems, liver tissue slices do not provide insights into the complex tissue-tissue interactions and excretion processes that are present in whole animals.

The expression and activities of hepatic P450 enzymes in naïve and inducer-treated rats have been well characterized. Briefly, earlier reports demonstrate that CYP2B1/2 and CYP3A2 expression and activities are lower in female rats, whereas no sex specific differences are observed for CYP1A2 (Asaoka et al., 2010). Furthermore, treatment with PB results primarily in an induction of CYP2B1 on both male and female rats (Lee et al., 1992; Nims et al., 1993; Waxman et al., 1985), whereas treatment with DEX induces CYP3A2 and CYP2B1 (Choudhuri et al., 1995; Meredith et al., 2003). qPCR analysis suggests analogous sex and inducer specific differences in P450 enzyme expression in the liver tissue slices employed in our study. Hashemi and co-workers have shown that the activity of P450 enzymes is also increased in tissue slices obtained from rats treated with classical inducers and that this activity decreases only slightly immediately after slice preparation (<4 h) (Hashemi et al., 2000).

In addition to hepatic metabolism, there is evidence that xenobiotics can be activated to toxic metabolites by P450 enzymes in different brain regions (Albores et al., 2001; Khokhar & Tyndale, 2012). One brain region implicated in PCB developmental neurotoxicity is the hippocampus (Wayman et al., 2012a,b); therefore, we used hippocampal slice cultures derived from PND4 rat pups to examine tissue specific metabolism in the enantioselective oxidation of neurotoxic PCBs. As determined by qPCR, these hippocampal slice cultures expressed the same CYPs implicated in PCB metabolism as are found in the liver, and the expression of these P450 enzymes did not change significantly as a function of day *in vitro* over the time span used to assess PCB metabolism. Because qPCR only indirectly assesses P450 activity, further studies are necessary to determine changes of P450 enzyme levels and activities in hippocampal tissue slices with time.

The majority of PCB 136 was present in the incubation buffer in both liver and hippocampal tissue slice incubations; however, 13–25% of total PCB 136 was associated with liver tissue slices and, thus, available for subsequent metabolism. The amount of PCB 136 associated with hippocampal slice cultures was 13–14-times lower compared to liver tissue slices. This difference in tissue partitioning is in agreement with *in vivo* studies showing higher PCB levels in the liver compared to the brain of mammals and humans. These differences cannot be attributed to the presence of the blood-brain barrier because lipophilic compounds, such as PCBs, cross cell membranes by passive diffusion. Furthermore, different lipid levels in both tissues cannot explain comparatively low levels of PCBs in brain tissue. For example, there are no differences in the extractable lipid content in brain and liver in mice (Milanowski et al., 2010), whereas PCB levels are typically lower in brain compared to liver (Kania-Korwel et al., 2008c, 2012). Similarly, PCB levels in human liver are higher compared to brain levels, despite higher fat levels in the brain (Dewailly et al., 1999). Instead, the overall lower PCB levels in brain are likely due to the high content of polar lipids in brain tissue, which have a low affinity for PCBs (Dewailly et al., 1999).

In vitro studies demonstrate that PCB 136 enantiospecifically sensitizes RyRs, with only (−)-PCB 136 being active towards RyRs (Pessah et al., 2009). In the present study, enantioselective analysis revealed a slight enantiomeric enrichment of the RyR active (−)-PCB 136 in liver tissue slices prepared from PB- and DEX-treated rats. The direction as well as the extent of the enrichment of (−)-PCB 136 is consistent with earlier PCB 136 metabolism studies using recombinant CYP2B1 (Warner et al., 2009) or rat liver microsomes (Wu et al., 2011) as well as an *in vivo* disposition study (Kania-Korwel et al., 2008b). The enantiomeric enrichment was also independent of sex and inducer pretreatment, despite the sex- and inducer-specific differences in the expression of P450 genes. Similarly, the enantiomeric enrichment of PCB 136 in C57Bl/6 mice was independent of inducer treatment (Kania-Korwel et al., 2008c) and sex (Kania-Korwel et al., 2007) after oral administration of PCB 136 dose. However, (+)-PCB 136 was enriched in C57BL/6 mice (Kania-Korwel et al., 2007, 2008c).

OH-PCBs, which are also potent sensitizers of RyRs (Pessah et al., 2006), may play a role in the developmental neurotoxicity of PCBs. As with the parent PCBs, the effect of OH-PCBs on RyR sensitization may be enantiomer-specific and, thus, can be modulated by the enantioselective formation of OH-PCB 136 metabolites. Conventional GC analysis, which measures the sum of the two atropisomers of a chiral PCB metabolite, showed that 4-OH-PCB 136 was the major metabolite in tissue slices from CTL rats. 4-OH-PCB 136 is the major metabolite formed in human microsomal metabolism studies (Schnellmann et al., 1983). In contrast, 5-OH-PCB 136 was the major metabolite in tissue slices from PB- and DEX-treated rats, which is consistent with metabolism studies using rat liver microsomes (Wu et al., 2011). While 4-OH-PCB 136 levels were comparable in tissue slices obtained from PB-, DEX- and CTL animals, the formation of 5-OH-PCB 136 increased in the order CTL < DEX < PB. This rank order of 5-OH-PCB 136 levels is consistent with formation of 5-OH-PCB 136 by CYP2B enzymes (Waller et al., 1999; Warner et al., 2009), which are induced by PB- and, to a lesser extent, DEX-treatment (Kania-Korwel et al., 2008a; Wu et al., 2011).

Enantioselective GC analysis revealed that the atropisomers of both OH-PCB 136 metabolites were present at different levels in the tissue slice incubation, thus displaying an enantiomeric enrichment. Specifically, $E_{(2)}$-5-OH-PCB 136, which is formed from (+)-PCB 136 (Wu et al., 2011), displayed a pronounced enrichment in the tissue slice incubations. This preferential formation of $E_{(2)}$-5-OH-PCB 136 is consistent with the slight enrichment of (−)-PCB 136 in tissue slices from PB- and DEX treated-animals. In contrast to 5-OH-PCB 136, $E_{(1)}$-4-OH-PCB 136, which is formed from (−)-PCB 136 (Wu et al., 2011), was enriched in liver tissue slices. Similar enrichment patterns were observed in studies using rat liver microsomes and *in vivo* results (Kania-Korwel et al., 2008b; Wu et al., 2011). Interestingly, the extent and

direction of the enantiomeric enrichment of both OH-PCBs was independent of the inducer pretreatment and the sex.

The most intriguing observations of the present study are the sex-specific differences in the OH-PCB profiles and levels observed with conventional and enantioselective GC analysis. Specifically, OH-PCB levels were higher in liver slices obtained from male versus female rats, independent of the inducer treatment. The higher OH-PCB levels in liver slices from male rats are likely due to higher CYP2B activities in male compared to female rats. Since tissue slices are a good model to predict sex-specific differences in xenobiotic metabolism (Ohyama et al., 2005a, b), our findings suggest that male rats eliminate PCB 136 more rapidly than female rats, both in CTL animals and after induction of P450 enzymes. To the best of our knowledge, sex specific differences in the toxicokinetics of PCB congeners metabolized in the rat have not been studied to date.

Our observations raise the question of whether differences in hepatic CYP2B activity result in different profiles and levels of neurotoxic PCB atropisomers and their metabolites at the target site during developmentally sensitive periods. Such differences in toxicant levels may play a role in PCBs' developmental neurotoxicity and contribute to the sex-specific differences observed in developmental toxicity studies in rats (Roegge et al., 2000; Widholm et al., 2001). Since CYP2B6, the human ortholog of rat CYP2B1, is an inducible enzyme (Zanger et al., 2007), our findings also indicate that the susceptibility to neurodevelopmental effects of PCBs may be modulated by the highly variable activity of CYP2B6 in humans. Although it is still unclear to what extent sex influences the expression of CYP2B6 (Zanger et al., 2007), further studies are warranted to investigate a potential role of hepatic PCB metabolism by CYP2B6 in the sex specific neurodevelopmental effects following PCB exposure in humans.

Although PCB 136 was associated with hippocampal tissue slices, OH-PCB 136 metabolites levels in hippocampal slice cultures were below background levels, which may reflect the low constitutive expression of CYP2B1/2 enzymes in mammalian brains (Volk et al., 1995) or, similar to liver tissue slice cultures (Hashemi et al., 2000), the loss of P450 enzyme activity with incubation time. To date, OH-PCBs have been detected in the brain of cetaceans (Kunisue et al., 2007), polar bears (Gebbink et al., 2008) and rats (Meerts et al., 2002), whereas OH-PCB levels were below the detection limits in mice exposed subchronically to PCB 95 (Kania-Korwel et al., 2012). The OH-PCBs in the brain are typically lower than in liver because OH-PCBs are more protein than lipid associated (Gebbink et al., 2008). Overall, additional studies using more sensitive analytical tools are needed to investigate levels and enantiomeric enrichment of chiral OH-PCBs in brain.

Conclusions

The present study demonstrates that both sex and the induction of P450 enzyme influence the metabolism of PCB 136 atropisomers in rat liver tissue slices and that the brain is apparently not a major site of PCB 136 metabolism. Although further studies are needed, our results suggest that sex and induction status of P450 enzymes in the liver may modulate the neurotoxic outcomes of developmental exposures to chiral PCBs.

Acknowledgements

The authors would like to thank Ananya Pramanik and Jarline Encarnacion Medina for help with liver slice incubations and E.A. Mash and S.C. Waller of the Synthetic Chemistry Facility Core of the Southwest Environmental Health Sciences Center for providing the PCB 136 derivatives.

Declaration of interest

This project was supported by the National Institute of Environmental Health Sciences (grants ES05605, ES013661 and ES017425). Hao Chen and Marianna Stamou were supported by a fellowship from the UC Davis Superfund Basic Research Program (grant ES04699). The synthesis of the PCB 136 derivatives was also funded by National Institute of Environmental Health Sciences (grant ES06694). The content of the manuscript is solely the responsibility of the authors and does not necessarily represent the official views of the National Institute of Environmental Health Sciences or the National Institutes of Health. The authors report no conflict of interest.

References

Albores A, Ortega-Mantilla G, Sierra-Santoyo A, et al. (2001). Cytochrome P450 2B (CYP2B)-mediated activation of methyl-parathion in rat brain extracts. Toxicol Lett 124:1–10.

Asaoka Y, Sakai H, Sasaki J, et al. (2010). Changes in the gene expression and enzyme activity of hepatic cytochrome P450 in juvenile Sprague-Dawley rats. J Vet Med Sci 72:471–9.

Black TH. (1982). The preparation and reactions of diazomethane. Aldrichim Acta 15:3–10.

Brown JF, Lawton RW, Ross MR, et al. (1989). Persistence of PCB congeners in capacitor workers and yusho patients. Chemosphere 19: 829–34.

Choudhuri S, Zhang XJ, Waskiewicz MJ, Thomas PE. (1995). Differential regulation of cytochrome P450 3A1 and P450 3A2 in rat liver following dexamethasone treatment. J Biochem Toxicol 10: 299–307.

Dammanahalli JK, Duffel MW. (2012). Oxidative modification of rat sulfotransferase 1A1 activity in hepatic tissue slices correlates with effects on the purified enzyme. Drug Metab Dispos 40:298–303.

Dewailly E, Mulvad G, Pedersen HS, et al. (1999). Concentration of organochlorines in human brain, liver, and adipose tissue autopsy samples from Greenland. Environ Health Perspect 107:823–8.

Dutta SK, Mitra PS, Ghosh S, et al. (2012). Differential gene expression and a functional analysis of PCB-exposed children: understanding disease and disorder development. Environ Int 40:143–54.

Fisher RL, Vickers AE. (2013). Preparation and culture of precision-cut organ slices from human and animal. Xenobiotica 43:8–14.

Gebbink WA, Sonne C, Dietz R, et al. (2008). Tissue-specific congener composition of organohalogen and metabolite contaminants in East Greenland polar bears (Ursus maritimus). Environ Pollut 152:621–9.

Hashemi E, Till C, Ioannides C. (2000). Stability of cytochrome P450 proteins in cultured precision-cut rat liver slices. Toxicology 149: 51–61.

Hu D, Hornbuckle KC. (2010). Inadvertent polychlorinated biphenyls in commercial paint pigments. Environ Sci Technol 44:2822–7.

Hu D, Lehmler HJ, Martinez A, et al. (2010). Atmospheric PCB congeners across Chicago. Atmos Environ 44:1550–7.

Hu D, Martinez A, Hornbuckle KC. (2011). Sedimentary records of non-Aroclor and Aroclor PCB mixtures in the Great Lakes. J Great Lakes Res 37:359–64.

Inoue K, Harada K, Takenaka K, et al. (2006). Levels and concentration ratios of polychlorinated biphenyls and polybrominated diphenyl ethers in serum and breast milk in Japanese mothers. Environ Health Perspect 114:1179–85.

Ioannides C. (2013). Up-regulation of cytochrome P450 and phase II enzymes by xenobiotics in precision-cut tissue slices. Xenobiotica 43: 15–28.

Kania-Korwel I, Barnhart CD, Stamou M, et al. (2012). 2,2′,3,5′,6-Pentachlorobiphenyl (PCB 95) and its hydroxylated metabolites are enantiomerically enriched in female mice. Environ Sci Technol 46:11393–401.

Kania-Korwel I, Duffel MW, Lehmler HJ. (2011). Gas chromatographic analysis with chiral cyclodextrin phases reveals the enantioselective formation of hydroxylated polychlorinated biphenyls by rat liver microsomes. Environ Sci Technol 45:9590–6.

Kania-Korwel I, Hrycay EG, Bandiera SM, Lehmler HJ. (2008a). 2,2′,3,3′,6,6′-Hexachlorobiphenyl (PCB 136) atropisomers interact enantioselectively with hepatic microsomal cytochrome P450 enzymes. Chem Res Toxicol 21:1295–303.

Kania-Korwel I, Shaikh N, Hornbuckle KC, et al. (2007). Enantioselective disposition of PCB 136 (2,2′,3,3′,6,6′-hexachlorobiphenyl) in C57BL/6 mice after oral and intraperitoneal administration. Chirality 19:56–66.

Kania-Korwel I, Vyas S, Song Y, Lehmler HJ. (2008b). Gas chromatographic separation of methoxylated polychlorinated biphenyl atropisomer. J Chromatogr A 1207:146–54.

Kania-Korwel I, Xie W, Hornbuckle KC, et al. (2008c). Enantiomeric enrichment of 2,2′,3,3′,6,6′-hexachlorobiphenyl (PCB 136) in mice after induction of CYP enzymes. Arch Environ Contam Toxicol 55: 510–7.

Khokhar JY, Tyndale RF. (2012). Rat Brain CYP2B-enzymatic activation of chlorpyrifos to the oxon mediates cholinergic neurotoxicity. Toxicol Sci 126:325–35.

Kunisue T, Sakiyama T, Yamada TK, et al. (2007). Occurrence of hydroxylated polychlorinated biphenyls in the brain of cetaceans stranded along the Japanese coast. Mar Pollut Bull 54:963–73.

Lake BG, Price RJ. (2013). Evaluation of the metabolism and hepatotoxicity of xenobiotics utilizing precision-cut slices. Xenobiotica 43:41–53.

Lee YS, Park SS, Kim ND. (1992). Sex-related differences in rat hepatic cytochromes P450 expression following treatment with phenobarbital or 3-methylcholanthrene. Arch Pharm Res 15: 78–86.

Lehmler HJ, Harrad SJ, Hühnerfuss H, et al. (2010). Chiral polychlorinated biphenyl transport, metabolism, and distribution: a review. Environ Sci Technol 44:2757–66.

Lehmler HJ, Robertson LW, Garrison AW, Kodavanti PRS. (2005). Effects of PCB 84 enantiomers on [^{3}H] phorbol ester binding in rat cerebellar granule cells and $^{45}Ca^{2+}$-uptake in rat cerebellum. Toxicol Lett 156:391–400.

Lein PJ, Barnhart CD, Pessah IN. (2011). Acute hippocampal slice preparation and hippocampal slice cultures. Methods Mol Biol 758: 115–34.

Liu M, Oyarzabal EA, Yang R, et al. (2008). A novel method for assessing sex-specific and genotype-specific response to injury in astrocyte culture. J Neurosci Methods 171:214–17.

Lowry OH, Rosenbrough NJ, Rarr AL, Randall RJ. (1951). Protein measurement with Folin Phenol reagent. J Biol Chem 193:265–75.

Mariussen E, Fonnum F. (2006). Neurochemical targets and behavioral effects of organohalogen compounds: an update. Crit Rev Toxicol 36: 253–89.

Meerts IA, Assink Y, Cenijn PH, et al. (2002). Placental transfer of a hydroxylated polychlorinated biphenyl and effects on fetal and maternal thyroid hormone homeostasis in the rat. Toxicol Sci 68: 361–71.

Meredith C, Scott MP, Renwick AB, et al. (2003). Studies on the induction of rat hepatic CYP1A, CYP2B, CYP3A and CYP4A subfamily form mRNAs in vivo and in vitro using precision-cut rat liver slices. Xenobiotica 33:511–27.

Milanowski B, Lulek J, Lehmler H-J, Kania-Korwel I. (2010). Assessment of disposition of chiral polychlorinated biphenyls in female mdr 1a/b knockout versus wild-type mice using multivariate analyses. Environ Int 36:884–92.

Naik RS, Mujumdar AM, Ghaskadbi S. (2004). Protection of liver cells from ethanol cytotoxicity by curcumin in liver slice culture in vitro. J Ethnopharmacol 95:31–7.

Nelissen K, Smeets K, Mulder M, et al. (2010). Selection of reference genes for gene expression studies in rat oligodendrocytes using quantitative real time PCR. J Neurosci Methods 187:78–83.

Nims RW, Lubet RA, Jones CR, et al. (1993). Comparative pharmacodynamics of CYP2B induction by phenobarbital in the male and female F344/NCr rat. Biochem Pharmacol 45:521–6.

Ohyama K, Maki S, Sato K, Kato Y. (2005a). Comparative *in vitro* metabolism of methoxychlor in male and female rats: metabolism of demethylated methoxychlor metabolites by precision-cut rat liver slices. Xenobiotica 35:683–95.

Ohyama K, Maki S, Sato K, Kato Y. (2005b). Comparative *in vitro* metabolism of the suspected pro-oestrogenic compound, methoxychlor in precision-cut liver slices from male and female rats. Xenobiotica 35:331–42.

Park JS, Bergman A, Linderholm L, et al. (2008). Placental transfer of polychlorinated biphenyls, their hydroxylated metabolites and pentachlorophenol in pregnant women from eastern Slovakia. Chemosphere 70:1676–84.

Pessah IN, Hansen LG, Albertson TE, et al. (2006). Structure-activity relationship for noncoplanar polychlorinated biphenyl congeners toward the ryanodine receptor-Ca^{2+} channel complex type 1 (RyR1). Chem Res Toxicol 19:92–101.

Pessah IN, Lehmler HJ, Robertson LW, et al. (2009). Enantiomeric specificity of (−)-2,2′,3,3′,6,6′-hexachlorobiphenyl toward ryanodine receptor types 1 and 2. Chem Res Toxicol 22:201–7.

Pessah IN, Cherednichenko G, Lein PJ. (2010). Minding the calcium store: ryanodine receptor activation as a convergent mechanism of PCB toxicity. Pharmacol Therap 125:260–85.

Pfaffl MW. (2001). A new mathematical model for relative quantification in real-time RT-PCR. Nucleic Acids Res 29:2002–7.

Pfaffl MW, Horgan GW, Dempfle L. (2002). Relative expression software tool (REST) for group-wise comparison and statistical analysis of relative expression results in real-time PCR. Nucleic Acids Res 30:1–10.

Reed M, Fujiwara H, Thompson DC. (2001). Comparative metabolism, covalent binding and toxicity of BHT congeners in rat liver slices. Chem Biol Interact 138:155–70.

Rios LM, Jones PR, Moore C, Narayan UV. (2010). Quantitation of persistent organic pollutants adsorbed on plastic debris from the Northern Pacific Gyre's ''eastern garbage patch''. J Environ Monit 12: 2226–36.

Roegge CS, Seo BW, Crofton KM, Schantz SL. (2000). Gestational-lactational exposure to Aroclor 1254 impairs radial-arm maze performance in male rats. Toxicol Sci 57:121–30.

Sagiv SK, Thurston SW, Bellinger DC, et al. (2012). Neuropsychological measures of attention and impulse control among 8-year-old children exposed prenatally to organochlorines. Environ Health Perspect 120: 904–9.

Schnellmann R, Putnam C, Sipes I. (1983). Metabolism of 2,2′,3,3′,6,6′-hexachlorobiphenyl and 2,2′,4,4′,5,5′-hexachlorobiphenyl by human hepatic microsomes. Biochem Pharmacol 32:3233–9.

Shaikh N, Parkin S, Lehmler HJ. (2006). The Ullmann coupling reaction: a new approach to tetraarylstannanes. Organometallics 25:4207–14.

Su G, Liu X, Gao Z, et al. (2012). Dietary intake of polybrominated diphenyl ethers (PBDEs) and polychlorinated biphenyls (PCBs) from fish and meat by residents of Nanjing, China. Environ Int 42:138–43.

Thomas PE, Reik LM, Ryan DE, Levin W. (1983). Induction of two immunochemically related rat liver cytochrome P-450 isozymes, cytochromes P-450c and P-450d, by structurally diverse xenobiotics. J Biol Chem 258:4590–8.

Ulrich EM, Willett KL, Caperell-Grant A, et al. (2001). Understanding enantioselective processes: a laboratory rat model for alpha-hexachlorocyclohexane accumulation. Environ Sci Technol 35: 1604–9.

USEPA. (2013). Basic Information of polychlorinated biphenyl (PCB). Available from: http://www.epa.gov/osw/hazard/tsd/pcbs/pubs/about.htm [last accessed 11 Jan 2013].

Valentovic MA, Ball JG, Anestis DK, Rankin GO. (1995). Comparison of the in vitro toxicity of dichloroaniline structural isomers. Toxicol In Vitro 9:75–81.

Van den Berg M, Birnbaum LS, Denison M, et al. (2006). The 2005 World Health Organization reevaluation of human and mammalian toxic equivalency factors for dioxins and dioxin-like compounds. Toxicol Sci 93:223–41.

Volk B, Meyer RP, von Lintig F, et al. (1995). Localization and characterization of cytochrome P450 in the brain. In vivo and in vitro investigations on phenytoin- and phenobarbital-inducible isoforms. Toxicol Lett 82–83:655–62.

Waller SC, He YA, Harlow GR, et al. (1999). 2,2′,3,3′,6,6′-Hexachlorobiphenyl hydroxylation by active site mutants of cytochrome P450 2B1 and 2B11. Chem Res Toxicol 12:690–9.

Warner NA, Martin JW, Wong CS. (2009). Chiral polychlorinated biphenyls are biotransformed enantioselectively by mammalian cytochrome P-450 isozymes to form hydroxylated metabolites. Environ Sci Technol 43:114–21.

Waxman DJ, Dannan GA, Guengerich FP. (1985). Regulation of rat hepatic cytochrome P-450: age-dependent expression, hormonal imprinting, and xenobiotic inducibility of sex-specific isoenzymes. Biochemistry 24:4409–17.

Waxman DJ, Walsh C. (1982). Phenobarbital-induced rat liver cytochrome P-450. Purification and characterization of two closely related isozymic forms. J Biol Chem 257:10446–57.

Wayman GA, Bose D, Yang D, et al. (2012a). PCB 95 modulates calcium-dependent signaling pathway responsible for activity-dependent 1 dendritic growth. Environ Health Perspect 120:1003–9.

Wayman GA, Yang D, Bose DD, et al. (2012b). PCB 95 promotes dendritic growth via ryanodine receptor-dependent mechanisms. Environ Health Perspect 120:997–1002.

Widholm JJ, Clarkson GB, Strupp BJ, et al. (2001). Spatial reversal learning in Aroclor 1254-exposed rats: sex-specific deficits in associative ability and inhibitory control. Toxicol Appl Pharmacol 174:188–98.

Wu X, Pramanik A, Duffel MW, et al. (2011). 2,2′,3,3′,6,6′-Hexachlorobiphenyl (PCB 136) is enantioselectively metabolized to hydroxylated metabolites by rat liver microsomes. Chem Res Toxicol 24:2249–57.

Yang D, Kim KH, Phimister A, et al. (2009). Developmental exposure to polychlorinated biphenyls interferes with experience-dependent dendritic plasticity and ryanodine receptor expression in weanling rats. Environ Health Perspect 117: 426–35.

Zanger UM, Klein K, Saussele T, et al. (2007). Polymorphic CYP2B6: molecular mechanisms and emerging clinical significance. Pharmacogenomics 8:743–59.

Appendix

Table A1. Effect of treatment on body and liver weights of rats used to prepare liver tissue slices.

Inducer treatment	Sex	Final weight (g)	Percent change in body weight[a,$]	Liver weight (g)[a]	Liver-to-final body weight ratio[a]
Phenobarbital (PB)	Female ($n=3$)	224 ± 2	5.5 ± 1.3	10.1 ± 0.4	4.5 ± 0.2
	Male ($n=3$)	300 ± 20	-2.0 ± 7.0	16.0 ± 2.0	5.3 ± 0.9
DEX	Female ($n=3$)	186 ± 6	-12.0 ± 4.4*	12.1 ± 0.2*	6.5 ± 0.3*
	Male ($n=3$)	249 ± 4	-17.0 ± 0.7*	16.8 ± 0.6	6.8 ± 0.2*
CTL	Female ($n=3$)	219 ± 4	1.3 ± 3.2	9.2 ± 0.7	4.2 ± 0.3
	Male ($n=2$)	300 ± 30	0.0 ± 0.0	13.0 ± 2.0	4.4 ± 0.4

[a]Data are presented as the mean ± standard deviation. One-way ANOVA and *post hoc* Tukey's test (SAS software, version 9.3) were used for multiple comparisons.

[$]Percent change in body weight = (Final body weight – Initial body weight)/Initial body weight × 100.

*Significantly different from CTL ($p < 0.5$).

Table A2. Primer set sequences.

Gene	Forward primer	Reverse primer
cyp2B1/2	CAACCCTTGATGACCGCAGT	TGGAGAGCTGAACTCAGGATGGG
cyp3A2	AATGGAGCCTGACTTTCCCTCAAG	GCATCAAGAGCAGTCAATTAAGTCCAG
cyp1A2	ATGAAGCCCAGAACCTGTGAAC	GTATGGGTTTGCAGGGAACAGT
cyp4X1	AAACGGCACCTATGAGTCTTATG	TTGCCTAACTCCTGGAAGCA
cyp2S1	AGGACGTCCATTCAACCCTTCCAT	TCATAGGGCAAACGGATGCCAAAG

Table A3. The limit of detection (*LOD*) and background levels of PCB 136 and its hydroxylated metabolites in medium blanks and tissue slice samples not treated with PCBs.

Tissue slices	QA/QC Measure	PCB 136	5-OH-PCB136	4-OH-PCB 136	4,5-diOH-PCB 136
Liver tissue slice incubations	*LOD** (ng) ($n=19$)	49	11	8.5	1.4
	Medium from vehicle-treated incubations (1:200 DMSO) (ng/mL) ($n=20$)	6.4 ± 7.3	0.9 ± 2.1	0.7 ± 1.0	0.1 ± 0.1
	Tissue slices incubated in blank medium with vehicle (ng/mg) ($n=19$)	0.8 ± 1.0	0.1 ± 0.1	0.1 ± 0.1	0.1 ± 0.1
Hippocampal tissue slice incubations	*LOD** (ng) ($n=9$)	7.6	64	53	2.8
	Medium from vehicle-treated incubations (1:1000 DMSO) (ng/mL) ($n=7$)	6.3 ± 1.6	21 ± 10	33 ± 8	1.3 ± 1.2
	Tissue slices incubated in blank medium with vehicle (ng/incubation) or (ng/mg) ($n=7$)	5.7 ± 1.0 (0.6 ± 0.1)	3.5 ± 6.2 (0.4 ± 0.6)	14 ± 12 (1.4 ± 1.2)	0.4 ± 0.7 (0.1 ± 0.1)

PCB 136 and its hydroxylated metabolites were quantified using an Agilent 6890N GC with ^{63}Ni-μECD detector and a DB1-MS capillary column (60 m × 0.25 mm ID × 0.25 μm film thickness; Agilent, Santa Clara, CA). The temperature program was as follows: 100 °C for 1 min, 5 °C/min to 250 °C, hold for 20 min, 5 °C/min to 280 °C, hold for 3 min. The flow rate was 1 mL/min.

*The *LOD* in liver and hippocampal tissue slice incubations are based on blank samples containing buffer only. The *LOD* was calculated from blank samples as $LOD = \overline{x_b} + k \cdot s_b$, where $\overline{x_b}$ is the mean of samples, k is Student's t-value for $n-1$ degrees of freedom at 99% confidence level, and s_b is standard deviation of the blank measures (Kania-Korwel et al., 2007). The comparatively high *LOD* in hippocampal tissue slice incubations is likely due to the use of plastic ware (Rios et al., 2010).

Table A4. *LOD* and resolution (R_s) of the atropisomers of PCB 136 and its hydroxylated metabolites in rat liver slices.

	PCB 136 (ng)		5-OH-PCB 136 (ng)		4-OH-PCB 136 (ng)	
Parameter	(−)	(+)	$E_{(1)}$	$E_{(2)}$	$E_{(1)}$	$E_{(2)}$
LOD on Chirasil-Dex column	39.8 ($n=3$)	50.7 ($n=3$)	ND		NA	
LOD on Cyclosil-B column	NA		NA		5.3 ($n=3$)	5.1 ($n=3$)
R_s	0.73		0.61		0.74	

The *LOD* was calculated from blank samples as $LOD = \overline{x_b} + k \cdot s_b$, where $\overline{x_b}$ is mean of samples, k is Student's t-value for $n-1$ degrees of freedom at 99% confidence level, and s_b is standard deviation of the blank measures (Kania-Korwel et al., 2007). The R_s was calculated using the formula $R_s = (t_{R2} - t_{R1})/0.5(BW_1 + BW_2)$, where t_{R2} and t_{R1} are the retention times of the first and second eluting enantiomer, and BW_1 and BW_2 are the baseline width of the first and second eluting enantiomer (Kania-Korwel et al., 2008b). NA, not applicable. ND, not determined. A comparable study determined the *LOD* for $E_{(1)}$- and $E_{(2)}$-5-OH-PCB 136 to be 9.9 and 16.8 ng, respectively (Wu et al., 2011).

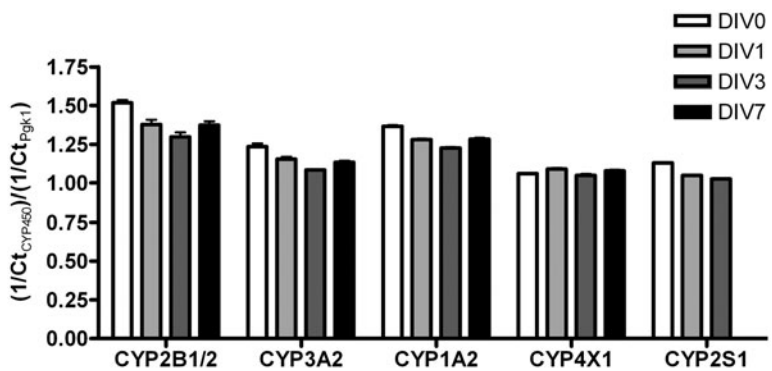

Figure A1. Cytochrome P450 transcript levels in rat hippocampal slices do not change significantly as a function of DIV. Slice cultures were obtained from hippocampi harvested from rats on postnatal day 4. Total RNA was collected after varying times in culture and mRNA levels quantified by qPCR. The Ct value for each individual cytochrome P450 gene was normalized to the Ct value for the reference gene (Pgk1) in the same sample. Data are presented as the mean ± S.E.M. ($n=3$ technical replicates of total RNA from a pooled sample of six hippocampal slices). CYP2S1 expression was not determined in DIV7 samples. No significant differences between treatment groups were detected by one-way ANOVA at $p<0.05$ (GraphPad Prism software).

Table A5. Protein and PCB 136 levels in liver tissue slices from naïve CTL, PB- or DEX-treated rats[a].

Inducer treatment	Sex	Protein levels[b] (mg)	PCB 136 in tissue slices [medium][&,$] (nmol)	PCB 136 in tissue slices (ng/mg protein)[&,$]	Recovery of total PCB 136 (%)[c]
PB	Female	18 ± 3	2.5 ± 0.4* [9.5 ± 0.5]*	53 ± 10*	120 ± 10
	Male	22 ± 4	1.3 ± 0.3 [8.6 ± 0.4]	21 ± 6	110 ± 10
DEX	Female	19 ± 3	2.1 ± 0.3 [6.7 ± 0.7]*	42 ± 14	91 ± 11
	Male	25 ± 3	1.8 ± 0.4 [5.7 ± 0.3]	27 ± 7	82 ± 9
CTL	Female	18 ± 2	2.4 ± 0.5 [8.5 ± 0.1]*	45 ± 15	109 ± 7
	Male	24 ± 4	2.3 ± 0.1 [6.3 ± 0.3]	33 ± 5	87 ± 14

Liver tissue slices from CTL, PB- or DEX-treated rats were incubated with PCB 136 (5 μM; 10 nmol per incubation sample) for 2 h at 37 °C as described under Materials and methods. Data are presented as the mean ± standard deviation ($n = 2$ or 3, with triplicate incubations; see also Table S1). PCB 136 was quantified using an Agilent 6890N GC with ^{63}Ni-μECD detector and a DB1-MS capillary column (60 m × 0.25 mm ID × 0.25 μm film thickness; Agilent, Santa Clara, CA). The temperature program was as follows: 100 °C for 1 min, 5 °C/min to 250 °C, hold for 20 min, 5 °C/min to 280 °C, hold for 3 min. The flow rate was 1 mL/min. [a] SAS software was used for the statistical analysis. Two way ANOVA with GLM and multiple comparisons were used to identify significant effects of sex and inducer pretreatment. [&] Inducer pretreatment had no overall effect on PCB 136 levels. [$] Amount of PCB 136 in liver slices was overall lower in male versus female rats ($p < 0.01$). * Significantly higher amount of PCB 136 in medium and/or slices in female than male rats ($p < 0.01$). [b] Protein levels in two pieces of liver slices after 2 h incubation. [c] The recovery of total PCB 136 (10 nmol PCB 136 added to each sample) was determined as the percentage of PCB 136 plus its metabolites (Table S4) detected in the tissue slices and medium after a 2 h incubation.

Table A6. Formation of hydroxylated PCB 136 metabolites in liver tissue slices from naïve CTL, PB- or DEX-treated rats.

		Metabolite formation								
			5-OH-PCB 136			4-OH-PCB 136			4,5di-OH-PCB 136		
Inducer treatment	Sex	ΣOH-PCB as percent of PCB 136[a]	Slices [medium] (pmol)	Slices (ng/mg protein)	Percent of ΣOH-PCB[a]	Slices [medium] (pmol)	Slices (ng/mg protein)	Percent of ΣOH-PCB[a]	Slices [medium] (pmol)	Slices (ng/mg protein)	Percent of ΣOH-PCB[a]
PB	Female	5.3 ± 1.1	490 ± 100 [ND]	11 ± 1.3	93 ± 1	30 ± 4 [ND]	0.7 ± 0.0	5.8 ± 1.0	6 ± 3 [ND]	0.1 ± 0.1	1.0 ± 0.4
	Male[b]	11 ± 2.7	900 ± 220 [115 ± 22]	16.0 ± 2.0	93 ± 4	15 ± 5 [ND]	0.3 ± 0.1	1.5 ± 0.2	32 ± 15 [24 ± 34]	0.6 ± 0.3	5.6 ± 3.6
DEX	Female	2.7 ± 1.3	240 ± 110 [ND]	4.9 ± 1.1	91 ± 4	24 ± 19 [ND]	0.5 ± 0.3	7.7 ± 3.5	3 ± 1 [ND]	0.1 ± 0.0	1.3 ± 0.3
	Male	6.1 ± 1.4	495 ± 95 [80 ± 37]	7.7 ± 1.2	95 ± 1	26 ± 5 [ND]	0.4 ± 0.1	4.3 ± 0.7	6 ± 2 [ND]	0.1 ± 0.0	0.9 ± 0.3
CTL	Female	0.5 ± 0.1	12 ± 10 [ND]	0.3 ± 0.2	25 ± 16	33 ± 4 [ND]	0.7 ± 0.1	75 ± 16	ND [ND]	ND	–
	Male	1.1 ± 0.4	50 ± 10 [ND]	0.7 ± 0.2	43 ± 5	60 ± 30 [ND]	1.0 ± 0.5	57 ± 5	ND [ND]	ND	–

Liver tissue slices from CTL, PB- or DEX-treated rats were incubated with PCB 136 (5 μM; 10 nmol per incubation sample) for 2 h at 37 °C as described under Materials and Methods. Data are presented as the mean ± standard deviation ($n = 2$ or 3, with triplicate incubations; see also Table S1). PCB 136 hydroxylated metabolites were quantified using an Agilent 6890N GC with ^{63}Ni-μECD detector and a DB1-MS capillary column (60 m × 0.25 mm ID × 0.25 μm film thickness; Agilent, Santa Clara, CA). The temperature program was as follows: 100 °C for 1 min, 5 °C/min to 250 °C, hold for 20 min, 5 °C/min to 280 °C, hold for 3 min. The flow rate was 1 mL/min. [a]Based on the amount of the respective metabolite in both tissue slices and medium. [b]Data from one incubation were excluded from the data analysis due to unacceptably low recoveries of the surrogate standard. ND, not detected.